Intermittency and Diffusion in the Hodgkin-Huxley Model

Gaspar Filipe Santos Magalhães Gomes Cano

Under supervision of Prof. Rui Manuel Agostinho Dilão

Non-Linear Dynamics Group

Department of Physics, IST, Lisbon, Portugal

April 2016

Abstract

We show that action potentials in the Hodgkin-Huxley neuron model result from a type I intermittency phenomenon that occurs in the proximity of a saddle-node bifurcation of limit cycles. For the Hodgkin-Huxley spatially extended model, describing the propagation of action potential along axons, we show the existence of type I intermittency and a new type of chaotic intermittency, as well as space propagating regular and chaotic diffusion waves. Chaotic intermittency occurs in the transition from a turbulent regime to the resting regime of the transmembrane potential and is characterised by the existence of a sequence of action potential spikes occurring at irregular time intervals.

Keywords: Hodgkin-Huxley model, type I intermittency, chaotic intermittency, diffusion waves.

1 Introduction

As nucleic acids are intrinsically negatively charged molecules, inside the cell, the zero charge balance is compensated by a non-zero concentration of positively charged ions. The transport of ions from the interior to the exterior of a cell and vice versa is done by ion channels and pumps. These channels and pumps are transmembrane proteins localised along the cellular membrane, [1], and are specific to the type of ion (Na^+, K^+, Cl^-, *etc.*) they carry. Channels perform passive transport, moving ions according to their concentration gradient, while pumps perform active transport, moving them against their concentration gradient, and keeping the balance of concentrations in check. There are two types of ion channels – gated and non-gated channels. Non-gated channels are always open, while gated channels may open or close as a function of some variable (e.g. the membrane potential). At equilibrium, a constant potential difference from the inside to the outside of the cell is kept [2].

The Hodgkin-Huxley (HH) neuron excitation model, [3–6], describes the potential drop across cell membranes due to the exchange of ions. This model has been introduced to describe patch clamp experiments on the giant

axon of the squid *Loligo*. The equations of the HH model are

$$\begin{aligned} C_m \frac{@V}{@t} &= D\frac{@^2V}{@x^2} \quad g_{\mathrm{Na}}m^3h(V \quad E_{\mathrm{Na}}) \quad g_{\mathrm{K}}n^4(V \quad E_{\mathrm{K}}) \quad g_{\mathrm{L}}(V \quad E_{\mathrm{L}}) \quad i \\ \frac{@n}{@t} &= \quad {}_n(V)(1 \quad n) \quad {}_n(V)n \\ \frac{@m}{@t} &= \quad {}_m(V)(1 \quad m) \quad {}_m(V)m \\ \frac{@h}{@t} &= \quad {}_h(V)(1 \quad h) \quad {}_h(V)h; \end{aligned} \tag{1}$$

where

$$\begin{aligned} {}_n &= 0{:}01\ \frac{V\ +\ 10}{e^{(V+10)=10}\quad 1}; \qquad {}_n = 0{:}125\ e^{V=80}; \\ {}_m &= 0{:}1\ \frac{V\ +\ 25}{e^{(V+25)=10}\quad 1}; \qquad {}_m = 4\ e^{V=18}; \\ {}_h &= 0{:}07\ e^{V=20}; \qquad\qquad {}_h = \frac{1}{e^{(V+30)=10}\quad 1}; \\ &= 3^{(T-6{:}3)=19}; \end{aligned} \tag{2}$$

In this model, V is the transmembrane potential drop measured in mV, i is a transmembrane current density, measured in A/cm^2 and time is measured in ms. The current density i is a transmembrane current density that is applied to the cell. For example, it can be an injected current in a patch clamp experiment, or the signal transmitted from other neurons through synapses. Ion channels open and close as a function of the potential difference between the inside and outside of cells. The gating variables n, m and h describe the opening and closing of the channel gates, are specific to the ion type and are dimensionless. The functional form of n, m and h in equations (1) has been proposed and calibrated in [6]. For a review of specific gating mechanisms associated to the choices made in equation (1), we refer to [1]. In equations (1), the ionic conductances across the cellular membrane are g_{Na} and g_{K}, and g_{L} is a constant measuring "leak" conductance. C_m is the membrane capacitance and D is a constant inversely proportional to the resistance ( ), measured along the axon of nerve cells. This model has been calibrated for the squid giant axon at the temperature $T = 6{:}3$ °C, [6], and the values of the constants are $C_m = 1$ F/cm^2, $g_{\mathrm{Na}} = 120$ mS/cm^2, $g_{\mathrm{K}} = 36$ mS/cm^2 and $g_{\mathrm{L}} = 0{:}3$ mS/cm^2, where S$=\ ^{-1}$ (siemens) is the unit of conductance. The Nernst equilibrium potentials, relating the difference in the concentrations of ions between the inside and the outside of cells with the transmembrane potential drop, are $E_{\mathrm{Na}} = \ 115$ mV, $E_{\mathrm{K}} = 12$ mV and $E_{\mathrm{L}} = \ 10{:}613$ mV. This choice of parameters is rescaled in such a way that at rest ($i = 0$), the steady state of the the transmembrane potential is $V^*(0) = 0$ mV. Hodgkin and Huxley have shown that the transmembrane diffusion coefficient is $D = a=(2R_2)$, where a is the radius of the axon (considered as a cylinder) and R_2 is the specific resistivity along the interior of the axon. For the case of the squid giant axon, $a = 238$ m, $R_2 = 35{:}4$ cm and $D = 3{:}4 \quad 10^{-4}$ S, [6]. The electrophysiological state of any cell can be described by a HH type model, provided its electric state is controlled by the opening and closing of voltage sensitive channels.

Assuming $D = 0$ in equations (1), the electrophysiological steady state is described by the vector quantity $p^*(i) = (V^*(i); n^*(i); m^*(i); h^*(i))$, where i is considered as an external parameter. If $i = 0$, for the (reference) parameter values described above, the steady state is stable and it is the unique limit set of the HH equations (1). As the position of the steady state $p^*(i)$ changes with i, due to its stability in the vicinity of $i = 0$, small

variations in the parameter i for a short period of time produce the same dynamic effects as changes in the initial conditions. These variations or changes may be considered as a perturbation of the steady state $p^*(0)$, which may or may not cause the neuron to fire – action potential response. The threshold that exists separating both cases can be described in the following way: consider a cell or neuron at the steady state $p^*(0)$; imposing a current density to the cell during some short time t_1, there exists a time interval t_{tr} and a threshold value I_{tr} such that, if $i(t)$ I_{tr}, for t_{tr} t m t_{tr}, with finite real $m > 1$, and $i(t) = 0$ otherwise, the system develops a spike in its voltage response $V(t)$ – the action potential. Then the voltage attenuates in time and the system returns to the stable steady state $p^*(0)$. If $i(t) < I_{tr}$, for t_{tr} t m t_{tr}, the voltage response $V(t)$ attenuates in time to the stable steady state $p^*(0)$ and the action potential does not develop. For the parameter region $D = 0$ and $i = 0$, the HH equations have a unique stable steady state (stable node) $p^*(0)$ in the four dimensional phase space. These simple facts are well known and discussed in the literature, [7], [8] and [2], among others.

One of the main goals of this work is to explain the origin of this threshold effect and the appearance of action potential spikes in the HH model equations and to characterise it dynamically. In the next section, we summarise the main dynamical properties of the solutions of the diffusion free ($D = 0$) HH equations (1). In section 3, we extend the concept of type I intermittency associated to saddle-node bifurcations of fixed points to intermittency of saddle-node bifurcation of limit cycles. We show that action potentials, as observed in the HH equation, are originated by this new type I intermittency. In section 4, we analyse the spatially extended HH model ($D > 0$) and show that a new type I spatial intermittency appears. In the presence of diffusion, sustained oscillations develop, as well as chaotic or turbulent action potential propagation. For high values of transmembrane current densities, turbulent action potentials disappear and the convergence to a stable steady state occurs mixed with intermittent action potential chaotic spikes. Finally, in section 5, we summarise the main conclusions of this work. The original research presented here has been submitted for publication [9].

2 A summary of the bifurcations of the diffusion free HH equation

In this analysis, all the parameters of equations (1) are kept fixed and the current density i is considered as the unique free parameter of the model. The majority of authors have done the numerical analysis of the HH equations (1) with the bifurcation analysis software AUTO, [10], and XPPAUT, [11]. The bifurcation diagram depicted in figure 1 summarises the main characteristics of the asymptotic solutions of the diffusion free HH equations ($D = 0$). The HH equations (1) have a unique fixed point with coordinates $p^*(i) = (V^*(i); n^*(i); m^*(i); h^*(i))$, whose position in phase space depends on i (the other parameters in (1) are kept fixed). The fixed point $p^*(i)$ has two Hopf bifurcations, one subcritical for $i = I_1$, and another supercritical for $i = I_2$. For $i > I_2$ and 0 $i < I_1$, the fixed point $p^*(i)$ is stable. For the parameter values in equations (1), $I_1 = 9{:}77$ A/cm^2 and $I_2 = 154{:}52$ A/cm^2. The local bifurcation analysis shows that for $i < I_1$ and I_1 i sufficiently small, the HH equations have at least two limit cycles, one stable and another unstable, [12] and [7]. The unstable limit cycle is created at I_1, for decreasing values of i, and the stable one is created at I_2, also for decreasing values of i. These two limit cycles collide at $i = I_0 < I_1$ and, for $i < I_0$ they do not exist. At $i = I_0 = 6{:}26$ A/cm^2, the HH equations have a saddle-node limit cycle bifurcation (SNLC), [13]. In this

analysis, we have considered the fixed reference temperature $T_e = 6.3$ C. However, for temperature T below 28.8 C, the overall behaviour of the bifurcation diagram is the same as the one in figure 1. The fixed point $p(i)$ is unstable for i in the interior of the interval $[I_1; I_2]$ and stable outside. The overall behaviour of the bifurcation diagram in figure 1a can be understood as a codimension 2 Bautin or generalised Hopf bifurcation, [13]. We assume that the knee" (figure 1b and [7]) of the bifurcation diagram that occurs in the interval $[I_3; I_4] = [7.84; 7.92]$ A/cm^2 does not affect the overall behaviour of the solutions of the HH equations. For T above 7.72 C, the parameters in equations (1) change and the dotted limit cycle curve in figure 1b loses its one-to-many feature. The chaotic behaviour conjectured in [14] occurs in the interval $[I_3; I_4]$, figure 1b. A period doubling effect on the period of the unstable limit cycle has also been reported in $[I_3; I_4]$, in [12] and [7], however this effect is not a period doubling codimension 1 bifurcation.

Figure 1: a) Bifurcation diagram for the diffusion free HH equations (1) as a function of the transmembrane current density parameter i. In the bifurcation diagram, we represent the stability of the coordinate $V(i)$ of the fixed point $p(i)$ and the maximum values of the $V(t)$-coordinate of the limit cycles (LC) associated with the Hopf bifurcations. Dotted lines correspond to unstable states and continuous lines to stable ones. The SNLC bifurcation occurs for $i = I_0 = 6.26$ A/cm^2, the subcritical Hopf bifurcation for $i = I_1 = 9.77$ A/cm^2 and the supercritical Hopf bifurcation for $i = I_2 = 154.52$ A/cm^2. b) Enlargement of the region in the neighbourhood of the knee" that occurs in the interval $[I_3; I_4] = [7.84; 7.92]$ A/cm^2. The bifurcation diagrams have been calculated with the software package XPPAUT.

For a review, recent references are [8] and [2].

3 Type I intermittency in the HH equations

We have established that for $D_V = 0$ and $i < I_0$, the equations only have one stable fixed point and asymptotically in time all the solutions converge to the steady rest state of the cell/neuron. However, when perturbed, the HH equations may still develop action potential responses for this region. In this parameter region ($i < I_0$), if the initial condition is away from the fixed point, let us say $p_0 = (V_0; n_0; m_0; h_0) \neq p(i)$, then the response of the system has two possible outcomes. If p_0 is close enough to $p(i)$, then the asymptotic solutions of the HH equations converge to $p(i)$, without ever doing a long excursion through phase space regions away from the fixed point. On the contrary, if p_0 is sufficiently displaced form $p(i)$ in the $(V; n; m; h)$ four-dimensional phase space, the solution of the HH equations does a large excursion in phase space, resembling, during some time, an almost periodic orbit action potential response. These two regions in phase space are separated by a boundary or threshold. As the parameter i approaches I_0 and p_0 is sufficiently displaced from $p(i)$, the larger are the number of transient spikes that appear in the potential V. For the same $i < I_0$, it is

possible to produce zero, one, or more spikes, depending on how far p_0 is from $p(i)$. There is, however, an upper limit for which, no matter how much we continue to displace p_0 from $p(i)$, no more spikes are produced. Thus, there is a maximum number of obtainable spikes for each $i < I_0$. Depending on the value of p_0, the number of spikes generated must be either equal to or below this maximum. These solutions of the HH equations are action potential type responses and, as we shall see now, they are the result of a type I intermittency phenomenon, [15], [16] and [17], near the codimension 2 SNLC bifurcation.

To show that this transient time behaviour corresponds to type I intermittency, we analyse the behaviour of the solutions of the HH equations near the SNLC bifurcation at $i = I_0$ (figure 1). It can be shown ([9]) that the intermittency characteristic of the SNLC codimension 2 bifurcation has the same scaling behaviour in the bifurcation parameter as the type I intermittency observed in interval maps, [15] and [16]. To be more specific, with $\varepsilon = I_0 - i$, the permanence time of the orbits of the HH equations (1) in the vicinity of the limit cycle that appears at the SNLC bifurcation ($\varepsilon = 0$) is $t_{per} = c/\sqrt{\varepsilon}$, where c is a constant. Denoting by P the period of the shadow limit cycle responsible for the spiky action potential response and by N the number of action potential spikes generated before the system goes to the rest steady state, we have $NP = t_{per}$, implying that

$$\ln N = C - \frac{1}{2}\ln \varepsilon; \tag{3}$$

where C is a constant.

The first test showing that the action potential solutions of the HH equations are associated with type I intermittency is to verify that the maximum number of action potencial spikes developed in the solution of the HH equations obeys the scaling relation (3). A second test of type I intermittency is to show that, close to the SNLC bifurcation, the maximum amplitude of each action potential spike, as a function of the maximum amplitude of the previous one, has a parabolic profile. This graph will be called the next amplitude map, [15].

Figure 2: SNLC intermittency for the HH model. a) Logarithm of the number of spikes N of the action potential in the left vicinity of the SNLC bifurcation, as a function of the logarithm of $\varepsilon = I_0 - i$. The slope of the fitted line is $s = -0.505$, in agreement with (3). b) Next amplitude map for the HH model, for the parameter value $i = 6.259$ A/cm^2, or $\varepsilon = 0.001$. V_N is the maximum value of the action potential spike number N. At the SNLC bifurcation, $\varepsilon = 0$, the parabolic profile shown touches the dotted line $V_{N+1} = V_N$.

In figure 2a, we show the number of spikes of the action potential generated by the HH equation, in the left vicinity of the SNLC bifurcation, as a function of $\varepsilon = I_0 - i$. For $\varepsilon \in [0.00030, 0.07532]$ the slope of the fit is $s = -0.505$, in agreement with the estimate (3). In figure 2b, we calculate the next amplitude map, where we

observe the typical parabolic pro le associated with type I intermittency. The main conclusion of this analysis is that the di usion free ($D = 0$) HH equations (1) exhibit type I intermittency in the left vicinity of the SNLC bifurcation. This intermittency phenomenon is responsible for the action potential spiky signals. The threshold is associated with a boundary in phase space that separates the two possible types of transient solutions. Our numerical analysis shows that for $i \in [0; I_0)$ and if the electrophysiological state of the cell is su ciently far from the steady state, the HH model always shows an intermittent response, with one or several action potential spikes.

4 Oscillatory and turbulent solutions of the HH equations

The HH equations (1) with spatial term $D > 0$ describe the axonal propagation of the potential function, as well as the opening and closing of ion channels. We consider a 1-dimensional domain of length L representing the axon. In the interior of the spatial domain, there is no transmembrane current excitation, but at the boundary $x = 0$ the neuron is excited with some (transmembrane) current density $i(t)$. Under these conditions, the HH equations (1) are rewritten in the form

$$\begin{aligned}
\frac{\partial V}{\partial t} &= D\frac{\partial^2 V}{\partial x^2} + F(V,\vec{z}) \quad \frac{1}{C_m}i(t), \quad \text{for} \quad x = 0, \\
\frac{\partial V}{\partial t} &= D\frac{\partial^2 V}{\partial x^2} + F(V,\vec{z}), \quad \text{for} \quad x \in (0, L), \\
\frac{\partial \vec{z}}{\partial t} &= G(V,\vec{z}), \quad \text{for} \quad x \in (0, L),
\end{aligned} \tag{4}$$

where x is measured in cm and t in ms. The last three equations in (1) have been collapsed into the third equation in (4). The vector functions F and G are de ned by comparison between equations (4) and (1) and $D = D/C_m$. We further consider that the transmembrane potential and the gate variables obey Neumann or zero ux boundary conditions $\frac{\partial V}{\partial x}_{x=0,L} = 0$ and $\frac{\partial \vec{z}}{\partial x}_{x=0,L} = 0$. The di usion term in (4) does not change the stability of the steady state $p(0)$, and a linear analysis leads to the conclusion that the homogeneous steady state of the extended HH equation is stable. However, away from the steady state, the situation can be di erent.

As the local dynamics of the HH model has intermittent solutions, we have analysed numerically how intermittency and di usion a ect the propagation of the action potential along the axon. To simulate the reaction-di usion equations (4) we have used a benchmarked numerical method, [18], obeying the discrete conservation law $\Delta x = \sqrt{6D\Delta t}$, where Δx and Δt are space and time discretisation steps. This relation between space and time steps minimizes the integration error. We have chosen the axon length $L = 50$ cm, with the spatial region divided into $M = 400$ small intervals of length Δx, where $L = M\Delta x$. As $D = \Delta x^2/(6\Delta t) = L^2/(6M^2\Delta t)$, we change Δt in the interval $[0.003, 0.033]$ ms, which corresponds to variations in the di usion coe cient in the interval $[0.23, 2.34]$ cm^2/ms. The value suggested by Hodgkin and Huxley, [6], is $D = 3.4 \times 10^{-4}$ S, giving $D = 0.34$ cm^2/ms, which is within the range of our numerical analysis. We have imposed a constant signal $i(t) = i_0$, for every $t \geq 0$, at $x = 0$. The initial condition along the axon was set to $p(0) = (V(0), n(0), m(0), h(0))$. We have found that, if the input transmembrane current density i_0 is above some threshold, the equations develop sustained oscillations as a result of the intermittency e ect of the di usion free HH equations for $i = 0$ (gure 2). If the input transmembrane current density at the axon

boundary is low, the resulting transmembrane potential along the axon converges to the steady state $p_e(0)$.

Further numerical simulations have shown that, for a certain range of the parameter i_0, the extended HH system (4) has spatial intermittency and periodic oscillations. In figure 3a, we depict in the $(i_0; D = \Delta x^2)$ parameter space (the realistic range $D \in [0.23, 2.34]$ cm^2/ms can also be represented as $D = \Delta x^2 \in [5; 50]$ ms^{-1}), the regions where both phenomena are observed. In figures 3b, 3c and 3d, we also look in detail at the time intervals between oscillations for the case $D = \Delta x^2 = 20$ ms^{-1}.

Figure 3: a) Bifurcation diagram of the HH extended model (4), as a function of the transmembrane current density i_0 at the axon boundary and of the diffusion coefficient $D = \Delta x^2$. We show two different types of intermittency, oscillations and spatial chaos (dark grey and dotted lines). b) Period (and time intervals) of the oscillatory solutions of the HH extended model (4), as a function of the current density i_0, for the diffusion coefficient $D = \Delta x^2 = 20$ ms^{-1}. The regions $[I_2; I_3]$ and $[I_4; I_5]$ are zoomed-in in (c) and (d), respectively.

In figure 3a, the black lines I_1 and I_5 delimit the regions where equations (4) show solutions with intermittency from regions with oscillatory and chaotic solutions. For parameters in the intermittency regions, the solutions of equations (4) show a finite number of spikes along the spatial domain before going to the stable steady state. The light and dark grey regions mark the solutions that are oscillatory and propagate through the spatial region. In the light grey region ($[I_1; I_2]$ and $[I_3; I_4]$), the time between successive spikes is always the same. Between the light dashed lines I_2 and I_3 the time interval between successive spikes is irregular (figure 3c) dark grey region. The light dashed line I_4 precedes the final line I_5 only by a couple of decimal places and marks the beginning of a chaotic region, characterised by the chaotic behaviour of the time intervals between successive action potential spikes (figure 3d), characteristic of chaotic maps of the interval.

We have also calculated the velocity of propagation of the action potentials for different values of the diffusion coefficient. For our realistic range of diffusion coefficients, the numerical values for velocity were found to be

between 6 and 20 m/s, which are of the same order of magnitude of the experimental velocity $v = 21.2$ m/s, measured by Hodgkin and Huxley in the giant axon of the squid *Loligo*, [6].

4.1 Type I spatial intermittency

In the region $i_0 < I_1^*$ of figure 3a, the HH model with diffusion has type I intermittency solutions. To characterise this intermittency, we have tested the parameter scaling and the next amplitude map as in section 3. In the intermittency regime, we have counted the number of action potential spikes that propagate along the domain $[0; L]$, and have calculated the next amplitude maps. In figure 4 we show the analogous of figure 2, now for the spatial HH equations, with $\varepsilon = I_1^* - i_0$ in the domain $\varepsilon \in [0.001; 0.231]$. The numerically determined slope of the scaling relation (3) is $s = -0.506$, in agreement with the theoretical prediction $s = -0.5$. The next amplitude map has been calculated for $i_0 = 56.010$ A/cm^2 $< I_1^* = 56.012$ A/cm^2 and $D = \chi^2 = 20$ cm^{-1}, showing a parabolic profile, characteristic of type I intermittency.

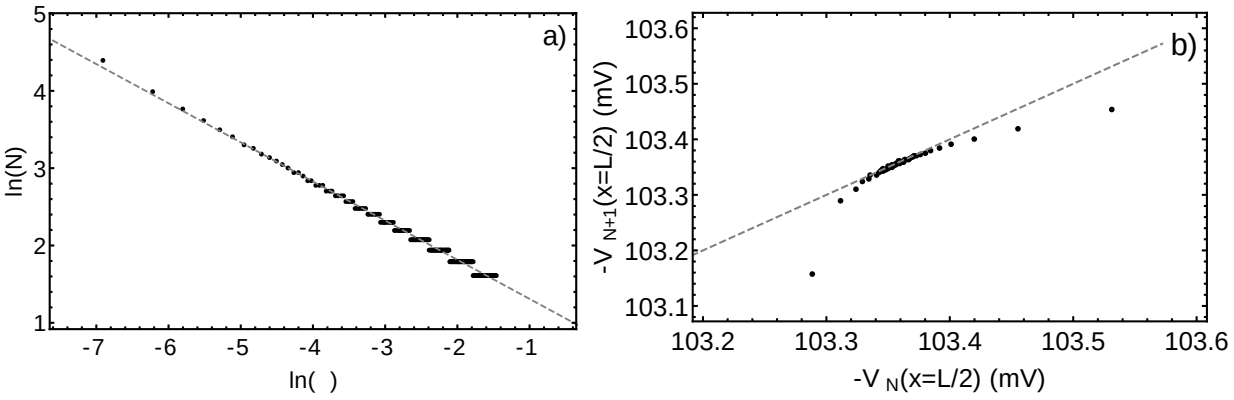

Figure 4: Type I intermittency for the HH extended model (4), with $D = \chi^2 = 20$ cm^{-1}. a) Logarithm of the number of spikes N of the action potential in the left vicinity of $I_1 = 56.012$ A/cm^2. The slope of the fitted dotted line is $s = -0.506$, in good agreement with (3). b) Next amplitude map for the parameter value $i_0 = 56.010$ A/cm^2 or $\varepsilon = 0.002$. $V_N(x = L/2)$ is the maximum value of the action potential spike number N, measured at the middle of the spatial domain $[0; L]$. The dotted line is the graph of the equation $V_{N+1} = V_N$.

4.2 Chaotic intermittency

A new intermittency of the HH extended model appears for $i_0 > I_5^*$. However, for this region, we have not found the same pattern we did in figures 2 and 4. In figure 5, we show the logarithm of the number of spikes as a function of the bifurcation parameter $\varepsilon = i_0 - I_5^*$, and the next amplitude map for the parameters $i_0 = 339.369$ A/cm^2, with diffusion coefficient $D = \chi^2 = 20$ cm^{-1}. From figure 5a, we conclude that the intermittent behaviour has no apparent scaling and is different from other types of intermittency. Indeed, the number of spikes as a function of the distance ε to the bifurcation point seems to behave randomly, without any scaling behaviour. Furthermore, the next amplitude map shown in figure 5b is not characteristic of any type of known intermittency phenomenon. Due to the irregular form of this map and the bifurcation diagram of figure 3d, we have called this phenomenon chaotic intermittency. These results have been submitted for publication [9].

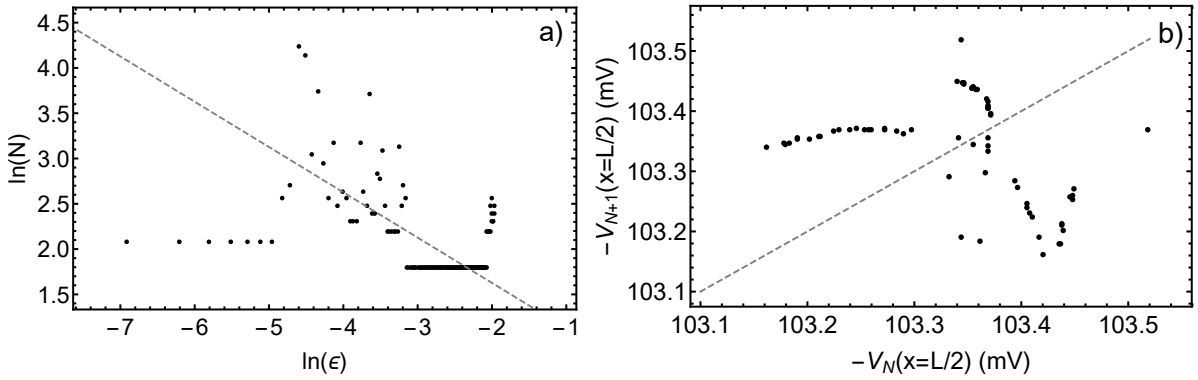

Figure 5: Chaotic intermittency for the HH extended model (4), with $D = x^2 = 20$ cm ^{1}. a) Logarithm of the number of spikes N of the action potential in the right vicinity of I_5, for $" = i_0 \quad I_5$ 2 [0:001; 0:140]. The dotted line has slope $s = 0{:}5$. b) Next amplitude map for the parameter value $i_0 = 339{:}369$ A/cm^2 or $" = 0{:}010$. $V_N(x = L{=}2)$ is the maximum value of the action potential spike number N, measured at the middle of the spatial domain $[0; L]$. Chaotic intermittency does not show any scaling behaviour on the number of spikes as a function of $"$. The dotted line is the graph of the equation $V_{N+1} = V_N$.

5 Conclusion

We have found the geometric and dynamical origins of the action potential type response of the Hodgkin-Huxley neuron model. This peculiar response is due to type I intermittency occurring in the vicinity of a saddle-node bifurcation of limit cycles. In this regime, neurons have a stable steady state but for large amplitudes of excitation they develop the action potential type of response, shadowing the existence of a stable limit cycle that appears at different parameter values. These conclusions were obtained under zero diffusion, implying that our results remain true for any cell with an electrophysiological state controlled by voltage sensitive channels.

We have extended our analysis to neurons with long axons. In this case, the diffusion coefficient of the HH model is positive and the solutions of the HH model equations show a more complex behaviour. For this case, we have assumed that neuron excitation is done at one boundary of the spatial domain through a transmembrane current. We have shown that, above some current density threshold, action potential spikes develop, showing type I intermittency characterised by a finite number of action potential spikes propagating along the axon. Increasing the values of the current density at the boundary of the axon, periodic propagating stable diffusion waves along the axon appear. In the parameter range of oscillations, we may have turbulent oscillations or chaos. These chaotic oscillations appear on the irregular time interval between successive action potential spikes and have a bifurcation diagram similar to the ones found in interval maps (figure 3d). For the parameter values where oscillatory or chaotic solutions exist, the steady state of the HH equations remains stable and is reached for small values of transmembrane current densities at the axon boundary. As far as we know, this is the first time that intermittency phenomena, chaotic or type I, are reported in an electrophysiological model of a cell. However, it is a common phenomenon found in electroencephalogram, [19], and epilepsia, [20].

Our analyses have been done for the original and calibrated HH model equations (1) and (4), with realistic diffusion coefficients. This implies that all the phenomena described here are predictions that can be explored in patch clamp experiments on giant axons. All the simulations are in agreement with HH observations, including the velocity of propagation of action potentials measured along the *Loligo* giant axon. The original research has been submitted for publication [9].

References

[1] J. P. Keener and J. Sneyd. *Mathematical physiology*. Springer, 1998.

[2] G. B. Ermentrout and D. H. Terman. *Mathematical foundations of neuroscience*. Springer, 2010.

[3] A. L. Hodgkin and A. F. Huxley. Currents carried by sodium and potassium ions through the membrane of the giant axon of Loligo. *The Journal of physiology*, 116(4):449, 1952.

[4] A. L. Hodgkin and A. F. Huxley. The components of membrane conductance in the giant axon of Loligo. *The Journal of physiology*, 116(4):473, 1952.

[5] A. L. Hodgkin and A. F. Huxley. The dual e□ect of membrane potential on sodium conductance in the giant axon of Loligo. *The Journal of physiology*, 116(4):497, 1952.

[6] A. L. Hodgkin and A. F. Huxley. A quantitative description of membrane current and its application to conduction and excitation in nerve. *The Journal of physiology*, 117(4):500, 1952.

[7] J. Rinzel and R. N. Miller. Numerical calculation of stable and unstable periodic solutions to the Hodgkin-Huxley equations. *Mathematical Biosciences*, 49:27–59, 1980.

[8] E. M. Izhikevich. *Dynamical systems in neuroscience*. MIT press, 2007.

[9] G. Cano and R. Dilão. Intermittency in the Hodgkin-Huxley model. *Preprint, http://preprints.ihes.fr/2016/M/M-16-06.pdf*, 2016.

[10] E. Doedel, H. B. Keller and J. P. Kernévez. Numerical analysis and control of bifurcation problems I. *Internat. J. Bifur. Chaos*, 1:493–520, 1991.

[11] B. Ermentrout. *Simulating, analyzing, and animating dynamical systems: a guide to XPPAUT for researchers and students*. SIAM, 2002.

[12] B. Hassard. Bifurcation of periodic solutions of the Hodgkin-Huxley model for the squid giant axon. *J. Theor. Biol.*, 71:401–420, 1978.

[13] Y. A. Kuznetsov. *Elements of applied bifurcation theory*. Springer, 3 edition, 2004.

[14] J. Guckenheimer and R. A. Oliva. Chaos in the Hodgkin-Huxley model. *SIAM J. Applied Dynamical Systems*, 1:105–114, 2002.

[15] Y. Pomeau and P. Manneville. Intermittent transition to turbulence in dissipative dynamical systems. *Comm. Math. Phys.*, 74:189–197, 1980.

[16] J. Guckenheimer and P. Holmes. *Nonlinear oscillations, dynamical systems, and bifurcations of vector fields*. Springer, 2002.

[17] J. Dias de Deus, R. Dilão and A. Noronha da Costa. Intermittency and sequences of periodic regions in one dimensional maps of interval. *Physics Letters A*, 101:459–463, 1984.

[18] R. Dilão and J. Sainhas. Validation and calibration of models for reaction-di□usion systems. *Internation Journal of Bifurcation and Chaos*, 8:1163–1182, 1998.

[19] A. D. Rae-Grant and Y. W. Kim. Type III intermittency: a nonlinear dynamic model of EEG burst suppression. *Electroencephalography and Clinical Neurophysiology*, 90:17–23, 1994.

[20] J. L. P. Velazquez, H. Khosravani, A. Lozano, B. L. Bardakjian, P. L. Carlen and R. Wennberg. Type III intermittency in human partial epilepsy. *European Journal of Neuroscience*, 11:2571–2576, 1999.